

# Receptor-mediated Endocytosis of Epidermal Growth Factor by Hepatocytes in the Perfused Rat Liver: Ligand and Receptor Dynamics

WILLIAM A. DUNN and ANN L. HUBBARD

*Department of Cell Biology and Anatomy, The Johns Hopkins University School of Medicine, Baltimore, Maryland 21205*

**ABSTRACT** We have used biochemical and morphological techniques to demonstrate that hepatocytes in the perfused liver bind, internalize, and degrade substantial amounts of murine epidermal growth factor (EGF) via a receptor-mediated process. Before ligand exposure, about 300,000 high-affinity receptors were detectable per cell, displayed no latency, and co-distributed with conventional plasma membrane markers. Cytochemical localization using EGF coupled to horseradish peroxidase (EGF-HRP) revealed that the receptors were distributed along the entire sinusoidal and lateral surfaces of hepatocytes. When saturating concentrations of EGF were perfused through a liver at 35°C, ligand clearance was biphasic with a rapid primary phase of 20,000 molecules/min per cell that dramatically changed at 15–20 min to a slower secondary phase of 2,500 molecules/min per cell. During the primary phase of uptake, approximately 250,000 molecules of EGF and 80% of the total functional receptors were internalized into endocytic vesicles which could be separated from enzyme markers for plasma membranes and lysosomes on sucrose gradients. The ligand pathway was visualized cytochemically 2–25 min after EGF-HRP internalization and a rapid transport from endosomes at the periphery to those in the Golgi apparatus–lysosome region was observed ( $t_{1/2} \cong 7$  min). However, no  $^{125}\text{I}$ -EGF degradation was detected for at least 20 min. Within 30 min after EGF addition, a steady state was reached which lasted up to 4 h such that (a) the rate of EGF clearance equaled the rate of ligand degradation (2,500 molecules/min per cell); (b) a constant pool of undegraded ligand was maintained in endosomes; and (c) the number of accessible (i.e., cell surface) receptors remained constant at 20% of initial values. By 4 h hepatocytes had internalized and degraded 3 and 2.3 times more EGF, respectively, than the initial number of available receptors, even in the presence of cycloheximide and without substantial loss of receptors. All of these results suggest that EGF receptors are internalized and that their rate of recycling to the surface from intracellular sites is governed by the rate of entry of ligand and/or receptor into lysosomes.

Receptor-mediated endocytosis (REM)<sup>1</sup> is well-recognized as a general mechanism used by many cells to take up biolog-

<sup>1</sup> *Abbreviations used in this paper:* APDE, alkaline phosphodiesterase; ASGP, asialoglycoprotein;  $\beta$ -NAG,  $\beta$ -N-acetyl-glucosaminidase; EGF, epidermal growth factor; EGF-HRP, conjugate of EGF to HRP, horseradish peroxidase; 5'-NUC, 5'-nucleotidase; Gal-Trans, galactosyl-transferase; LDL, low-density lipoprotein; RME, receptor-mediated endocytosis; SI, 0.25 M sucrose in 3 mM imidazole, pH 7.4; TCA, trichloroacetic acid; 12-K fraction, liver fraction sedimenting at 12,000 g.

ically important molecules. The variety of molecules taken up by RME include polypeptide hormones (e.g., epidermal growth factor [EGF] and insulin), transport proteins carrying nutritional and regulatory substances (e.g., low density-lipoprotein (LDL)-cholesterol, transcobalamin II-vitamin B12), lysosomal enzymes, asialoglycoproteins (ASGPs), and immunoglobulins (reviewed in reference 1). The destinations of these interiorized molecules vary from degradation in the lysosomal system with release of amino acids and monosaccharides (e.g., ASGP [2]) or of regulatory molecules (e.g., LDL

and cholesterol [1]) to intracellular sequestration in an undegraded form (e.g., yolk proteins [3]) to transport across the cytoplasm and subsequent exocytosis (e.g., immunoglobulins [3, 4]). The fates of the surface receptors interacting with specific ligands also vary from apparent reutilization during prolonged periods of activity (e.g., LDL and ASGP receptors [5, 6]) to loss of receptors after an initial wave of RME and subsequent desensitization of cells (e.g., hormonal "down-regulation" of EGF [7–11] or insulin [12, 13]). Thus, it is clear that eucaryotic cells carry out diverse functions that rely on the selective process of RME.

The principle cell in the liver, the parenchymal cell or hepatocyte, takes up many different molecules from the circulation via RME. These include ASGPs (2, 14), insulin (15), glucagon (16), prolactin (17), EGF (9, 18), transcobalamin II (19), haptoglobin-hemoglobin complexes (20), hemopexin-iron (21), glycoproteins with oligosaccharide chains terminating in  $\alpha$ 1,3 fucose residues (22), and immunoglobulin A (4). All of these molecules are internalized via receptor-mediated processes occurring at the sinusoidal surface of the hepatocyte. In addition, the fates of the ligands and of their receptors appear to encompass all currently established fates in RME. Therefore, the hepatocyte is particularly suitable for a comparative study of selected ligand-receptor systems, each having a different fate.

In recent years, we have been studying various aspects of ASGP endocytosis by hepatocytes (14, 23–26). This RME system represents one in which the ligand is ultimately delivered to and degraded within lysosomes but the receptor is reused. Hepatocytes also endocytose and degrade substantial amounts of EGF from the circulation but, unlike the ASGP receptor, they appear to down-regulate the EGF receptor. There is some evidence in cultured cells that the EGF receptor is delivered to lysosomes and degraded together with the ligand. However, no correlation has yet been made between the amount of EGF processed by these cells and the number of receptors lost.

Using the perfused liver, we have examined the kinetics of EGF uptake and degradation and the pathway of ligand entry from the cell surface to the lysosomes, both morphologically and biochemically. We have quantitated the amount of ligand internalized and degraded and compared these values with the number of receptors (i.e., nonlatent, latent, and total) present. Our results demonstrate that exposure to EGF induces a redistribution of hepatocyte receptor from the cell surface to an internal site (endosomes) but that these receptors are reutilized, since more ligand molecules are internalized than total functional receptors present, even when protein synthesis is inhibited. Portions of this study have been presented elsewhere in abstract form (27).

## MATERIALS AND METHODS

### Materials

Horseradish peroxidase (HRP, type VI), 3-amino-1,2,4-triazole, 3,3'-diaminobenzidine (grade II), polyethylene glycol (8,000 mol wt), and mannan were purchased from Sigma Chemical Co. (St. Louis, MO); HEPES was from Research Organics Inc. (Cleveland, OH); Brij 35 was from Pierce Chemical Co. (Rockford, IL); BSA, fraction V, was from Miles Laboratories Inc. (Elkhart, IN); and ultra-pure sucrose was obtained from Schwarz/Mann Inc. (Spring Valley, NY). Carrier-free  $\text{Na}^{125}\text{I}$  and uridine diphospho-D-[6- $^3\text{H}$ ]galactose were obtained from Amersham Corp. (Arlington Heights, IL). Male rats (CD strain) were supplied by Charles River (Wilmington, MA). All other reagents and compounds were of the highest purity available and were purchased from commercial sources.

### Preparation and Iodination of EGF

EGF was purified from male mouse submaxillary glands (Pel-Freez, Rogers, AR) as described by Savage and Cohen (28). Protein concentrations were calculated from the absorbance at 280 nm using an extinction coefficient at 10 mg/ml of 30.9 (29). EGF was iodinated by the chloramine T method (30) with resulting specific radioactivities of 20–150,000 cpm/ng.

### Isolated Perfused Liver System

Livers from 24-h fasted rats (150–250 g) were surgically removed and perfused in a recycling system with a balanced salt solution supplemented with 2% polyvinyl pyrrolidone-40 (26) and oxygenated with 95%  $\text{O}_2$ /5%  $\text{CO}_2$ .

**SURFACE BINDING OF EGF:** We quantitated exposed EGF receptors by recirculating a saturating dose of  $^{125}\text{I}$ -EGF (4–8  $\mu\text{g}$ , 6–12 nM) at 4°C and at periodic intervals removing 0.2–0.5 ml samples from the perfusing medium for determination of the radioactive content. After 90–120 min, the bound  $^{125}\text{I}$ -EGF was dissociated by addition of 5 ml of 1 M Na acetate pH 3.5, which lowered the medium pH to 5.0. The amount of EGF bound was quantitated either from the percent of radioactivity cleared from the perfusate, from the radioactivity present in a liver homogenate before acid treatment, or from the amount of bound radioactivity released when the perfusate was acidified. All three measurements yielded similar results. EGF binding capacity was expressed as micrograms of EGF bound per gram wet weight of liver and converted to receptors per hepatocyte using  $1.38 \times 10^8$  hepatocytes/g wet wt of liver (31) and assuming a 1:1 interaction for the ligand-receptor complex.

**ENDOCYTOSIS AND METABOLISM OF EGF:** 10–25  $\mu\text{g}$  (15–38 nM) of  $^{125}\text{I}$ -EGF was recirculated at 37°C for 4–240 min, and at timed intervals acid-soluble and insoluble radioactivity was determined in 0.2–0.5-ml aliquots of perfusate (see below). After terminating the uptake by cooling the liver to 4°C, we removed surface-bound EGF by acidifying the perfusing medium as described above and subsequently re-equilibrating the liver with cold, fresh perfusate. For subcellular fractionations, the liver was disconnected from the perfusion system before acidification, weighed, and homogenized. In vitro binding assays were performed on liver biopsies (0.3–0.5 g) excised before ligand addition and after removal of surface-bound ligand.

### In Vitro EGF Binding Assay

EGF binding was measured in vitro (32) on aliquots of liver homogenates (1.5–2 mg protein), subcellular fractions (1–2 mg protein), and fractions obtained from sucrose gradients. Samples were incubated with saturating doses (80 nM) of  $^{125}\text{I}$ -EGF (20–100,000 cpm/ng) for 60 min at 4°C in a total volume of 0.2 ml that contained 20 mM HEPES, pH 7.4, and 0.5% BSA. Since maximal EGF binding was observed within 30 min, these assay conditions represent steady-state. Binding was terminated by the sequential addition of 0.5 ml of 0.1% bovine IgG in 0.1 M phosphate buffer, pH 7.4, and 0.5 ml of 25% polyethylene glycol. The precipitated EGF-receptor complex was collected under gentle vacuum on Whatman GF/C filters (Whatman Laboratory Products Inc., Clifton, NJ) soaked in 0.1% BSA in 20 mM HEPES, pH 7.4, the filters were washed with 15 ml of 10% polyethylene glycol in 0.1 M phosphate buffer pH 7.4, and the radioactivity was retained on the filters measured. The difference between  $^{125}\text{I}$ -EGF binding in the absence and presence of a 50-fold molar excess of unlabeled EGF was taken as specific binding. Nonspecific binding ranged between 10 and 20% of total radioactivity bound and was <1% of the total radioactivity added to the incubation. With liver homogenates, binding capacity was expressed as micrograms of EGF bound per gram of liver or per milligram of protein. The number of receptors per cell was determined as described above or by using a calculated conversion factor of  $1 \times 10^6$  hepatocytes/mg protein based on the wet weight of unperfused livers.

The difference between specific  $^{125}\text{I}$ -EGF-binding sites measured in the presence (total) and absence (accessible) of detergent was defined as latent EGF receptors. As described in Results, Brij 35 was the most effective detergent in exposing latent receptors (detectable only after exposure of livers to EGF, see Results). Detergent was added along with the ligand and at several concentrations in order to obtain maximal EGF binding. A concentration of 0.2% (wt/wt) was sufficient for sucrose gradient fractions, while a range of 0.4–0.7% (wt/wt) was necessary when homogenates or subcellular fractions were assayed.

### Preparation and Characterization of HRP Conjugated to EGF (EGF-HRP)

The procedure of Sell et al. (33) with modifications was used to couple the N-terminal amino group of EGF (containing trace amounts of  $^{125}\text{I}$ -EGF) to the carbohydrate portion of HRP. Uncoupled EGF was removed from the mixture by dialysis (Amicon PM-10 Amicon Corp., Danvers, MA). Using this procedure

ture, 22% of the added  $^{125}\text{I}$ -EGF was coupled to the HRP, and the final product retained at least 50% of the initial peroxidase activity (34). Analysis on SDS polyacrylamide gels revealed that 82% of the radiolabel migrated with an apparent molecular weight of 45,000 which was coincident with the major stained band and similar in electrophoretic mobility to the uncoupled HRP. The remaining radioactivity was distributed between a polypeptide at 90 kdaltons (14%), which presumably represented HRP dimers plus at least one EGF, and uncoupled EGF at 6 kdaltons (4%).

$^{125}\text{I}$ -EGF-HRP binding measured in vitro with liver homogenates was specific and had an apparent dissociation constant of 15 nM, which is within the range determined for unconjugated  $^{125}\text{I}$ -EGF (Fig. 1). Inclusion of mannan had no effect, indicating that there was no binding in homogenates via the HRP moiety.

### Localization of EGF-HRP in the Perfused Liver and Quantitation of HRP-containing Structures

EGF-HRP (4  $\mu\text{g}$  of EGF) was perfused through a liver at 4°C for 120 min. 5 mg of mannan was included as a precaution to inhibit binding of the conjugate via the HRP moiety to mannose/*N*-acetyl-glucosamine receptors on nonparenchymal cells (14). Unbound ligand was removed and the liver was either immediately fixed by perfusion with 2% glutaraldehyde in 0.1 M sodium cacodylate, pH 7.4, or warmed to >30°C for 2–25 min and then fixed. Peroxidase activity in the fixed liver was visualized using the method of Wall et al. (25). The presence of EGF-HRP in specific regions of the hepatocyte cytoplasm (as defined in reference 25) was quantitated either at the microscope or on electron micrographs by counting the number of structures (regardless of size) containing HRP reaction product.

### Subcellular Fractionation of Liver Homogenates

Livers were weighed and homogenized in 5 vol of 0.25 M sucrose in 3 mM imidazole buffer, pH 7.4 (SI), and the following fractions were prepared (Beckman centrifuge, 60 Ti rotor, Beckman Instruments Inc., Palo Alto, CA): a 12,000  $g_{\text{max}}$  (10 min) pellet (12-K fraction), a 145,000  $g_{\text{max}}$  (90 min) pellet (microsomal fraction), and a 145,000  $g_{\text{max}}$  (90 min) supernate (cytosolic fraction) (35). The 12-K pellet was resuspended in SI (5 ml/g liver) using a loose Dounce homogenizer and 5 ml (65–85 mg of protein) was applied to the top of a linear 1.11–1.25 g/cc sucrose gradient (32 ml). The microsomal pellet was resuspended in 15 ml of SI with a Potter-Elvehjem homogenizer, and 5 ml (50–60 mg of protein) was applied to a 1.06–1.20 g/cc linear sucrose gradient (28 ml) that was made above a 4 ml cushion of 1.22 g/cc sucrose. After centrifugation of both gradients for 12–15 h at 83,000  $g_{\text{av}}$  in an SW28 Beckman rotor, 1.2-ml fractions were collected from the top using a Buchler Auto Densi-Flow fractionator (Buchler Instruments Inc., Fort Lee, NJ).

### Analytical Procedures

Perfusate and liver homogenates (0.3–0.5 ml) were precipitated with 10% trichloroacetic acid (TCA) in the presence of 0.2–1% BSA at 4°C for 60 min. The samples were centrifuged (3,000 rpm for 15 min), supernate and pellet were separated, and the radioactivity in each was determined in a Beckman Gamma 4000 counter. Acid-soluble radiolabeled products released by the liver into the perfusion medium were further analyzed by column chromatography. Sephadex G-25 medium (PD-10 columns, Pharmacia Inc., Piscataway, NJ) equilibrated with 1 M acetic acid was used to separate free iodide from iodotyrosine derivatives (36).

Protein was determined in triplicate following the procedure of Bradford (37) using BSA as standard. 5'-nucleotidase (5'-NUC) was assayed by measuring the release of phosphate from adenosine monophosphate (38). Alkaline phosphodiesterase (APDE) and  $\beta$ -*N*-acetyl-glucosaminidase ( $\beta$ -NAG) activities were determined following published procedures (38). Galactosyltransferase (Gal-Trans) was assayed by monitoring the incorporation of [ $^3\text{H}$ ]-galactose into ovalbumin (39).

## RESULTS

### Properties of EGF Binding

We first examined EGF binding in the isolated perfused liver at 4°C (Fig. 1). Binding of EGF was both saturable and reversible. Saturation occurred at EGF concentrations of 6–8 nM and yielded a maximum of 150,000 receptors per hepatocyte (see below for cell type identification). The apparent

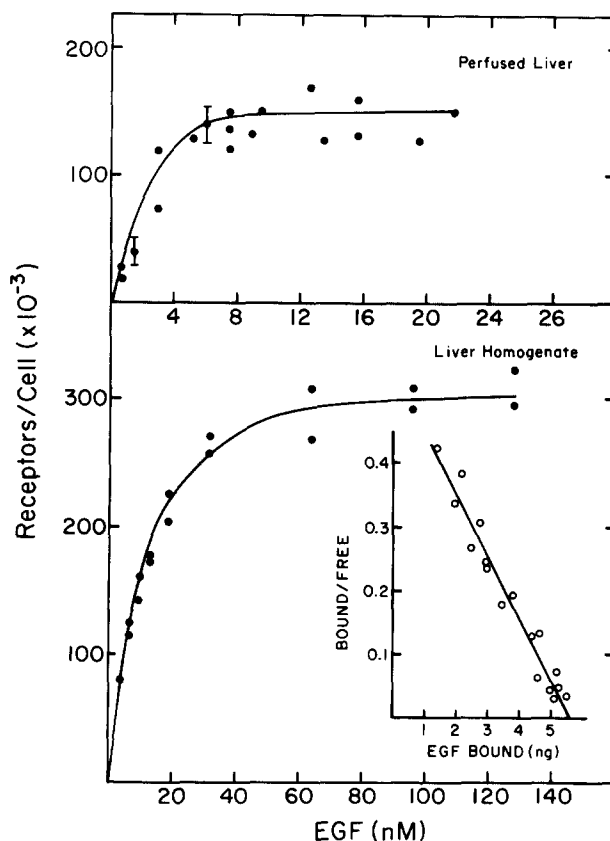


FIGURE 1 Binding of  $^{125}\text{I}$ -EGF in the isolated perfused liver and in a liver homogenate. The indicated concentrations of  $^{125}\text{I}$ -EGF were either perfused through livers (top panel) or incubated with liver homogenates (bottom panel) at 4°C for 60–90 min. The amount of EGF bound was then determined as described in Materials and Methods and expressed as receptors per cell. A Scatchard plot of the data obtained from liver homogenates is shown in the inset. The straight line plot was computer fitted to the experimental values (40). A similar plot for the perfused liver data could not be drawn because each determination was done on livers of various weights (5–9 g) which resulted in significant differences in total receptors measured per ligand concentration. An EGF concentration of 80 nM was necessary to saturate the high-affinity sites in liver homogenates and therefore was routinely used throughout this study to determine total available receptors in vitro. When standard error bars are present, the value is an average  $\pm$  SEM of at least five measurements. All other data points represent a single determination.

dissociation constant was 1–2 nM. When a 50-fold excess of unlabeled EGF was added at 4°C, 90% of the  $^{125}\text{I}$ -EGF previously bound was displaced with a  $t_{1/2}$  of 60 min. Dissociation of bound ligand was also pH dependent and occurred rapidly ( $t_{1/2} = 2$ –3 min) in the absence of excess EGF or calcium ions. At pH 6, 50% of the prebound ligand was released, while 90% was removed at pH 4.5–5.5 (Fig. 2A). Therefore, acid treatment (pH 5.0) for 10 min at 4°C was used as a measure of surface-bound EGF. This treatment had no significant effect on cell morphology (data not shown) nor on subsequent EGF binding (Fig. 2B) or uptake.

We next characterized EGF binding in liver homogenates (Fig. 1) and found 300,000 high-affinity sites of  $K_d = 8$ –15 nM by Scatchard analysis with no low-affinity sites (Fig. 1, inset). In addition, we found that 10–20% of the available binding sites in a liver homogenate were unstable to storage

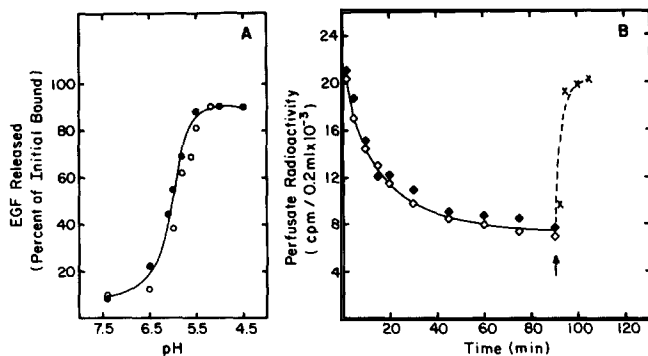


FIGURE 2 The effects of acid treatment on EGF binding in the perfused liver. The effect of pH on the release of prebound EGF (A) and on subsequent EGF binding (B) was examined in the perfused liver. (A)  $^{125}\text{I}$ -EGF (8 nM) was recirculated for 90 min through an isolated liver at 4°C, after which the perfusate was replaced with fresh medium (4°C) with (●) or without (○) 2.2 mM  $\text{CaCl}_2$  at the indicated pH. The buffers used were 20 mM HEPES (pH 7.4), 20 mM PIPES (pH 6.0–6.5), and 40 mM acetate or citrate (pH 5.0–5.8). The amount of EGF released at a particular pH was calculated from the increase in radioactivity in the medium after 15 min of perfusion and expressed as a percent of the radioactivity initially cleared from the perfusate and bound by the liver. (B) We examined the clearance of  $^{125}\text{I}$ -EGF (8 nM) at 4°C by taking aliquots of perfusate at selected times after the addition of ligand and measuring the radioactivity present (◆). Maximum binding of ligand by hepatocytes was achieved by 60–90 min at which time the medium was acidified to pH 5.0 by the addition of 5 ml of 1 M sodium acetate-buffered perfusate (pH 3.5) (arrow). After washing the liver free of acidic medium using fresh perfusate at 4°C, we added a second bolus of  $^{125}\text{I}$ -EGF and determined the clearance of ligand from the perfusion medium (◇).

on ice for 4–6 h or to freeze/thawing. For this reason binding assays were performed, when possible, on fresh homogenates.

In an effort to assay active receptors in a latent (intracellular) compartment, various detergents were screened for their ability to maintain EGF binding in liver homogenates (Fig. 3). The following detergents at final concentrations of 0.2–0.6% resulted in an almost total inhibition of EGF binding in the liver homogenate and were considered inappropriate for measuring intracellular receptors: digitonin, Triton X-100, 2-deoxycholate, Lubrol WX, and 3-[3-(cholamidopropyl) dimethylammonio]-1-propane-sulfonate (CHAPS). Only the nonionic detergent, Brij 35, at concentrations of 0.3–0.7%, had no effect on receptor number in homogenates of freshly isolated livers, but decreased receptor affinity ( $K_d = 25$  nM). The finding that Brij 35 did not increase the specific binding of  $^{125}\text{I}$ -EGF in freshly prepared liver homogenates, even at concentrations as low as 0.05%, suggested that all 300,000 receptors per cell were in an accessible compartment (i.e., at the cell surface).

### Cytochemical Localization of EGF in the Perfused Liver

EGF covalently coupled to HRP (EGF-HRP) was used to visualize the distribution of EGF binding sites at the cell surface (i.e., 4°C binding) and to investigate the route of ligand entry. At 4°C peroxidase reaction product was distributed along microvilli of the sinusoidal front and the lateral surface membrane of hepatocytes with some concentration in coated pit regions (Fig. 4). Although we did observe EGF-HRP binding to nonparenchymal cells, the reaction product was

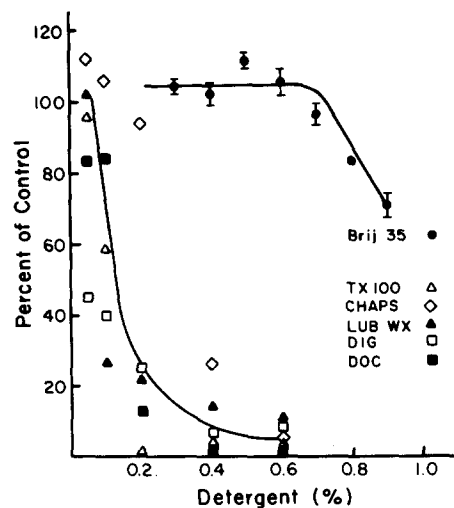


FIGURE 3 The effects of detergents on EGF binding in liver homogenates. Homogenates were incubated for 60 min at 4°C in the presence of 80 nM  $^{125}\text{I}$ -EGF and selected detergents at the indicated concentrations (wt/wt). Specific EGF binding was calculated as described in Materials and Methods and expressed as a percentage of EGF-binding capacity measured in the absence of detergent. When error bars are present, the value is an average  $\pm$  SEM of four to eight determinations. All other data points represent a single measurement. TX 100, Triton X-100; LUB WX, Lubrol WX; DIG, digitonin; DOC, 2-deoxycholate.

light and variable. When a 50-fold molar excess of EGF was perfused with EGF-HRP, the conjugate was not bound (as detected by the  $^{125}\text{I}$ -EGF moiety) and no HRP reaction product was observed on parenchymal or nonparenchymal cells.

To investigate the route of ligand entry into the cell, EGF-HRP was first perfused through a liver at 4°C. Unbound ligand was then washed away and the medium was rapidly warmed to 35°C for 2, 4, or 10–25 min. The HRP reaction product was almost exclusively associated with hepatocytes, demonstrating that liver parenchymal cells were responsible for the endocytosis of EGF. The HRP-positive structures were characterized morphologically (Fig. 5) and quantitated at selected times after warming (Table I). At 2 min, HRP product was predominantly localized in structures similar in size (50–100 nm) and shape to coated pits and vesicles (80% of the positive structures counted) (Table I and Fig. 5a). However, clathrin coats were not visible under the conditions of fixation and HRP visualization. Reaction product was absent from both the microvilli and lateral surfaces. By 4 min, HRP-positive structures included larger vesicles and tubules (100–200 nm diam) in addition to coated pits and vesicles (Fig. 5, b and c and Table I). These larger structures, which accounted for ~50% of the positive vesicles observed, were located at the cell periphery and were morphologically identical to type I endosomes as previously described for the endocytosis of ASGPs (41, 42). In fact, when EGF-HRP was perfused in the presence of asialoorosomuroid adsorbed to colloidal gold, 60–75% of the HRP-positive vesicles contained the gold tracer (A. L. Hubbard and W. A. Dunn, unpublished results). After 10–25 min of perfusion at 35°C, 66–85% of the vesicles containing HRP product were located in the Golgi apparatus-lysosome region of the cell (Fig. 5, d–f). These vesicles included small and large vesicles and tubules (type II endosomes, see references 41 and 42) and structures containing either lipoproteins or small vesicles (type III endosomes,

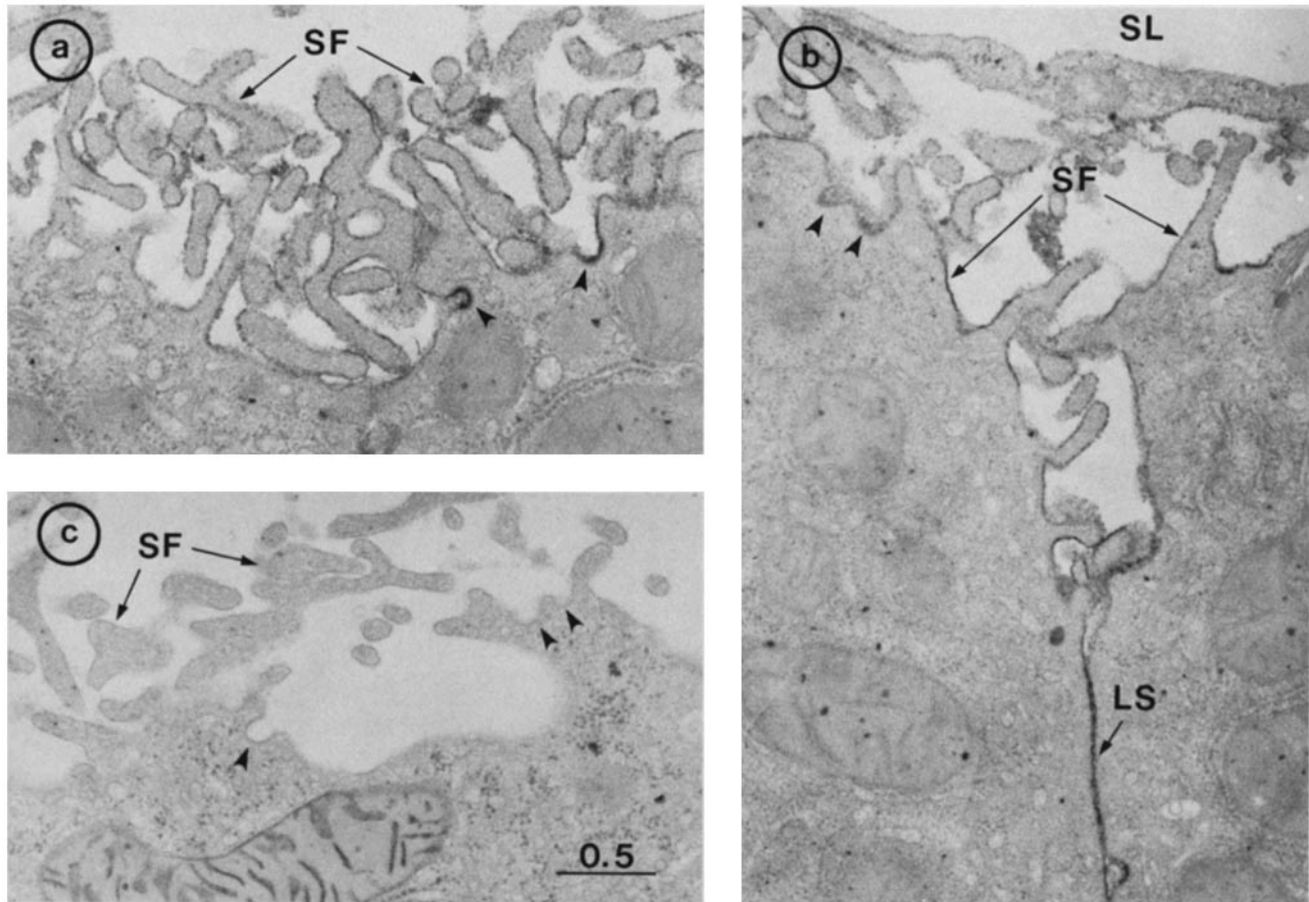


FIGURE 4 Surface distribution and specificity of EGF-HRP binding in the perfused liver. The distribution of EGF-HRP binding at 4°C to the cell surface was visualized as described in Materials and Methods (a and b). The reaction product was localized along microvilli of the sinusoidal front (SF), in coated pits (arrowheads), and along lateral surfaces (LS) of hepatocytes. Endothelial cells lining the sinusoidal lumen (SL) were found unlabeled. (c) When a 50-fold excess of unlabeled EGF was perfused along with EGF-HRP, no labeling of the hepatocyte plasma membrane was observed. Bar, 0.5  $\mu\text{m}$ . (a-c)  $\times 25,000$ .

references 41 and 42). At this time,  $^{125}\text{I}$ -EGF was not yet present in lysosomes but was still in a prelysosomal compartment as analyzed by subcellular fractionation (see below).

#### Kinetics and Extent of EGF Uptake

$^{125}\text{I}$ -EGF concentrations from 0.5–40 nM were continuously perfused through livers for up to 4 h and the disappearance of acid-insoluble radioactivity from the medium was monitored over time. The clearance curves of  $^{125}\text{I}$ -EGF at three representative concentrations are plotted in Fig. 6. At subsaturating levels (0.5 nM), >90% of the added  $^{125}\text{I}$ -EGF was cleared by 20 min. At intermediate and saturating EGF concentrations (5 and 20 nM) the clearance was biphasic, with a fast primary phase that abruptly changed at 15–20 min to a slower secondary phase. When the primary clearance phase (0–15 min) at these three concentrations was plotted semilogarithmically, straight lines were obtained (Fig. 6, inset). The rates of this initial uptake were calculated from the slopes and are presented in Fig. 7. From 0.06–1.5  $\mu\text{g}$  EGF/g liver, the rate of uptake increased concentrations of ligand. A double-reciprocal plot of the data indicated that the half-maximal clearance rate was obtained at 5 nM EGF. A maximal primary rate of 20,000 molecules/cell per min occurred at  $\sim 1.5$   $\mu\text{g}$  EGF added per gram liver (15 nM) and remained unchanged up to 4.0  $\mu\text{g}/\text{g}$  (40 nM).

When the added levels of EGF were  $\geq 0.5$   $\mu\text{g}/\text{g}$  (5 nM), the primary uptake was followed by a slower secondary clearance that was linear from  $\sim 30$  min to at least 240 min (Fig. 6). The rate of uptake increased with increasing ligand input to a maximal level of 2,500 molecules of EGF/min per cell at an EGF dose of  $\sim 1.4$   $\mu\text{g}/\text{g}$  liver (Fig. 7). This rate was 12–13% of that observed for the primary clearance and, as will be discussed below, equalled the rate of release of acid-soluble radioactivity from the liver.<sup>2</sup>

The amount of ligand internalized (i.e., inaccessible to acid release) as a function of time was quantitated using saturating doses of EGF ( $>1.4$   $\mu\text{g}/\text{g}$ ) and expressed on a per cell basis (Fig. 8). A rapid accumulation of 250,000 molecules/cell occurred during the first 20 min of EGF exposure. This was followed by a slower uptake of ligand which was linear for up to 4 h. The amount of EGF internalized at 4 h was three

<sup>2</sup> The secondary clearance phase was not due to EGF uptake by other cell types, since only hepatocytes possessed the ability to endocytose EGF. In addition, the secondary rate of uptake, although slower than the primary clearance, was rapid and saturable, two characteristics of receptor-mediated endocytosis, *not* fluid-phase pinocytosis (43). Finally, the difference between the primary and secondary rates of ligand uptake was not due to changes in EGF concentrations in the perfusate nor in receptor  $K_d$  values, but the result of a decrease in hepatocyte cell surface receptors.

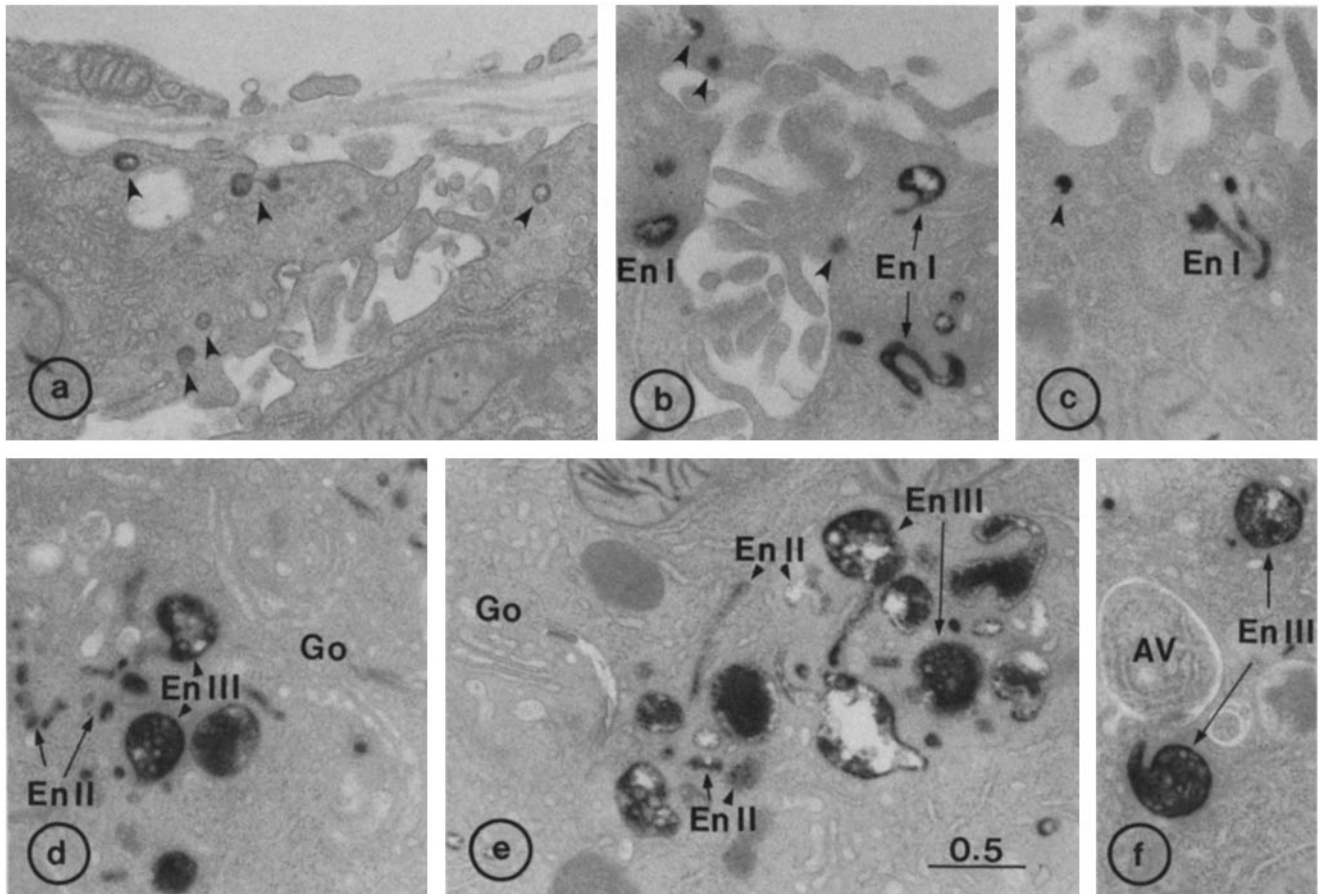


FIGURE 5 Intracellular localization of EGF-HRP in hepatocytes at 2 min (a), 4 min (b and c), and 10–25 min (d–f) after ligand internalization. An experimental protocol was used such that a single wave of EGF-HRP movement from the cell surface to the lysosomes could be visualized with time (see Materials and Methods). (a) 2 min after warming, EGF-HRP was near the plasma membrane in structures similar in dimensions to coated pits and vesicles (arrowheads). (b and c) By 4 min, HRP-positive structures included larger vesicles and tubules (type I endosomes, *En I*) in addition to coated pits and vesicles (arrowheads). (d–f) When the liver was warmed for 10–25 min, the HRP product was located in the Golgi-lysosome region of the cell in small and large vesicles and tubules designated endosomes type II (*En II*) and in structures resembling either lipoprotein-containing vesicles or multivesicular bodies, designated endosomes type III (*En III*). GO, Golgi apparatus; AV, autophagic vacuoles. Bar, 0.5  $\mu\text{m}$ . (a–f)  $\times 25,000$ .

times the total number of EGF binding sites in liver homogenates (Fig. 1). Cycloheximide (0.2–1 mM) at concentrations shown by others to inhibit protein synthesis in the perfused rat liver (44) had no effect on the amount of EGF internalized over a 4-h period.

#### Kinetics and Extent of EGF Degradation

No acid-soluble radioactivity appeared in the perfusate until 20 min, after which it increased linearly for up to 240 min (Fig. 6). Analysis by column chromatography revealed that the released radioactivity was free iodide. Since no significant accumulation of acid-soluble radioactivity was evident in the liver, we used the rate of increase of acid-soluble radioactivity in the perfusate to estimate the rate of hydrolysis of EGF by hepatocytes (Fig. 7).

As shown in Fig. 7, the rate of hydrolysis increased with EGF concentration up to  $\sim 1.4 \mu\text{g/g}$  liver (14 nM) and thereafter remained unchanged at a maximum of 2,500 molecules of EGF degraded/min per cell. By analyzing this data on a double-reciprocal plot (not shown), the EGF concentration necessary for a half-maximal degradative rate was 7 nM, which was comparable to that observed for the primary phase

of uptake (i.e., 5 nM).

The maximal rate of release of acid-soluble radioactivity from the liver was identical to the maximal rate observed for the secondary phase of EGF uptake, 2,500 molecules/cell per min, suggesting establishment of a steady state. Indeed, as shown in Fig. 8, after 20 min of perfusion with saturating levels of EGF ( $>1.4 \mu\text{g/g}$ ), a steady state was reached such that the amount of EGF internalized paralleled that which was degraded. The difference between the amount of EGF internalized and degraded remained constant from 20 to 240 min and represented an intracellular pool of  $\sim 200,000$  ligand molecules/cell, which was comparable to the amount of EGF internalized in the initial uptake phase, from 0–20 min.

Finally, we measured the amount of EGF hydrolyzed under saturating conditions. These results are presented in Fig. 8. After the initial 20-min lag, the amounts of EGF degraded increased linearly to a total of 690,000 molecules/cell at 4 h. This represents 2.3 times more ligand than the initial number of total available receptors measured in the liver homogenate. In addition, the amount of EGF degraded within 4 h was unaltered when protein synthesis was inhibited by 0.2–1 mM cycloheximide.

TABLE I  
Endocytosis of Surface-bound EGF-HRP by Hepatocytes at 32°C

Time of warming to 31–32°C min	Total structures counted	Intracellular Region*			
		Pits and small vesicles† %	En I‡ %	En II‡ %	En III‡ %
2	173	81	19		
4	527	28	49	18	5
10	539	9	25	54 (23)‡	12 (66)
15	459	12	16	56 (72)	16
25	344	4	11	50 (85)	35

\* The number of structures containing EGF-HRP in the indicated regions of the hepatocyte was determined without regard to size, and the percent distribution was calculated.

† This category contains structures of size (50–100 nm) and shape similar to those of coated pits and vesicles. However, clathrin coats were not visible under the conditions of fixation and HRP visualization; therefore, some type I endosomes, En I, may have been included in this category.

‡ Endosomes were classified as type I (peripheral vesicles and tubules <200 nm diam); type II, En II, (small vesicles and tubules in the Golgi-lysosome region; and type III, En III, (large, >200 nm diam) vesicles in the Golgi-lysosome region usually containing distinguishable smaller vesicles or other inclusions). (Refer to Fig. 5.)

§ Sum of endosomes type II and III.

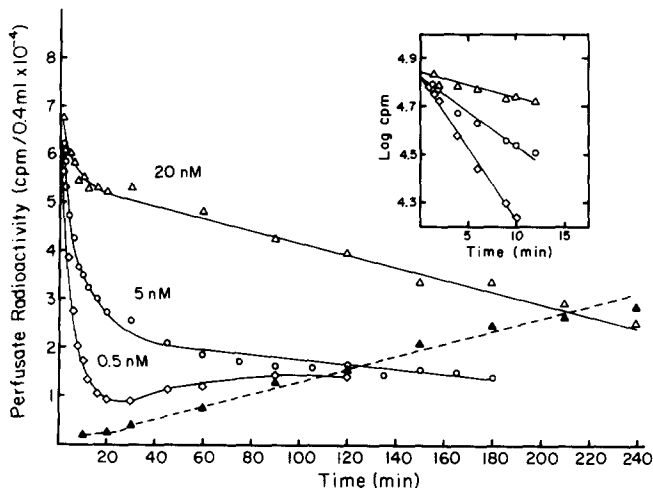


FIGURE 6 Clearance at 37°C of different concentrations of <sup>125</sup>I-EGF from the perfusion medium and accumulation of acid-soluble radioactivity in the perfusate. At the indicated times after addition of 0.5 nM (90,000 cpm/ng) (○), 5 nM (9,000 cpm/ng) (○), or 20 nM (2,250 cpm/ng) (△, ▲) <sup>125</sup>I-EGF, aliquots of perfusate were removed and precipitated with TCA as described in Materials and Methods, and the acid-insoluble radioactivity (open symbols) was plotted. When the primary rapid clearance phase at each concentration was plotted using the log of the radioactivity, straight lines were obtained with linear regression correlations of 0.96 ± 0.03 (inset). The acid-soluble radioactivity (▲) released from a liver exposed to 20 mM ligand accumulated in the circulating medium as a function of time after a lag of 20 min.

### Fate of EGF Receptor during Endocytosis

At selected times after addition of saturating doses of EGF, livers were homogenized and homogenates were assayed for accessible (minus Brij 35) and latent receptors (plus Brij 35)

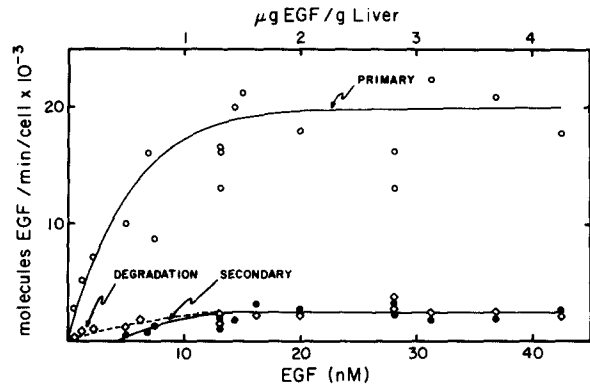


FIGURE 7 The effect of EGF concentration on the rates of primary and secondary clearance and on the rate of release of degradation products. Selected concentrations of <sup>125</sup>I-EGF were recirculated through perfused livers for up to 4 h and the clearance of ligand and subsequent release of radiolabeled products was measured. The rate of the primary clearance phase at each concentration was determined by multiplying the ligand input by the slope of a semilog plot of the acid-insoluble radioactivity in the perfusate at 0–15 min (Fig. 6, inset). The rates of the secondary clearance phase and of degradation were calculated from the specific radioactivities of the ligand and the slopes of the linear plots of the acid-insoluble and soluble radioactivity, respectively, in the perfusate from 30–240 min (Fig. 6).

as described in Materials and Methods. These results are presented in Fig. 8. Prior to EGF exposure the number of accessible and total receptors was the same, indicating the absence of a substantial intracellular pool. However, in the presence of EGF, a rapid decrease in accessible binding activity was observed which was coincident with an increase in latent binding.<sup>3</sup> Total binding activity (accessible plus latent) remained constant for up to 2 h and then declined to 70% of initial values by 4 h.

Between 4 and 20 min after EGF addition, when ligand was being rapidly internalized but not yet degraded, there was a progressive and rapid loss of up to 80% of the accessible binding activity (Fig. 8).<sup>4</sup> This decrease in accessible receptors coincided in time and amount with both an increase in latent binding activity and with the internalization of EGF. For example, when 250,000 molecules of EGF had been internalized per cell by 20 min, the number of accessible receptors decreased and that of latent receptors increased by approximately 200,000 per cell (65–70% of total).

At times longer than 20 min, when the rates of internalization and degradation of EGF had reached steady state, the number of accessible receptors remained constant at 50–60,000 receptors per cell, which represented 20% of the receptors initially accessible (Fig. 8). This 80% reduction coincided with a similar reduction in the rate of EGF uptake observed

<sup>3</sup> Accessible (nonlatent) receptors are those EGF-binding sites measured in the absence of Brij 35 detergent and are presumed to be located at the cell surface (see Results). Total functional receptors are determined in the presence of detergent and equal the sum of the accessible and latent receptors present. Latent receptors are presumed to be oriented towards the lumen of intact vesicles and thus incapable of binding added EGF without detergent permeabilization.

<sup>4</sup> EGF binding at 4°C in the perfused liver showed a trend similar to that seen for accessible receptors (i.e., 85% decrease within 20–60 min) but always yielded values that were 40–50% of those calculated in vitro in the absence of detergent.



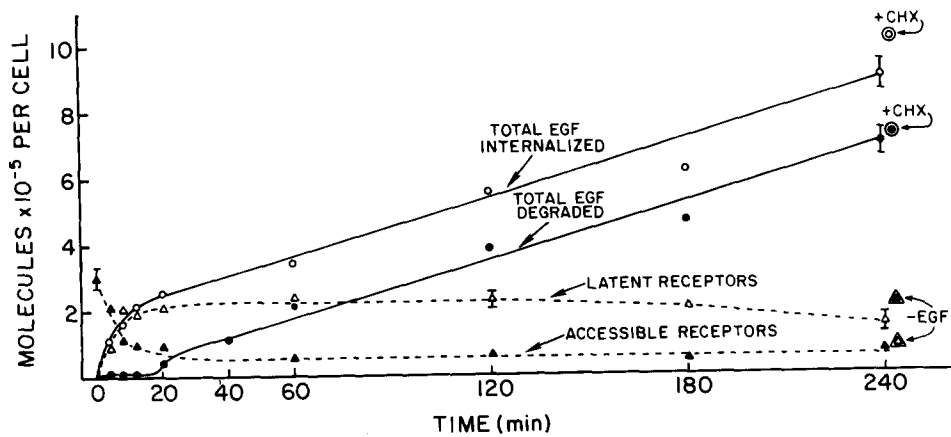


FIGURE 8 The uptake and degradation of EGF and effects on receptor number. At selected times (4–240 min) after the addition of saturating amounts of  $^{125}\text{I}$ -EGF ( $>1.4 \mu\text{g/g}$ ), whole livers and/or biopsies were homogenized in SI. Total acid-insoluble and -soluble radioactivity in the perfusate and liver was determined as described in Materials and Methods. Total EGF internalized (○) equaled TCA-soluble radioactivity in the perfusate plus total radioactivity in the liver. Combined TCA-soluble radioactivity in the liver and

perfusate yielded the total EGF degraded (●). Cycloheximide (CHX; ⊙, ⊙) at concentrations of 0.2–1 mM was perfused through a liver for 30 min prior to ligand addition. EGF binding capacity was measured in the absence (accessible; ▲) or presence (total) of 0.4–0.7% Brij-35 detergent (detergent to protein ratio of 0.4–1 [wt/wt]) as described in Materials and Methods. Latent receptors (Δ) were calculated from the difference in total and accessible receptors. To insure optimal recovery of latent receptors, we routinely used four to six detergent concentrations for each determination. Measurements of EGF binding capacity involved assaying unoccupied receptor sites in homogenates of livers that had previously been exposed to  $^{125}\text{I}$ -EGF. However, any potential problems introduced by the presence of sequestered ligand were eliminated by the assay conditions. This was accomplished using  $^{125}\text{I}$ -EGF of 10-fold higher specific activity and an amount that exceeded that of the sequestered ligand by a factor of ten. In addition, Brij 35 released at least 75% of the sequestered EGF within 60 min (the length of the incubation), thereby exposing latent receptors (data not shown). Thus, the presence of sequestered ligand did not interfere with an accurate measurement of total receptor number. The amount of EGF bound per aliquot was converted to receptors per cell using  $1.38 \times 10^8$  cells/g liver or  $1 \times 10^6$  cells/mg protein. Since the liver retained interstitial fluid with time of perfusion (26), we found it necessary to standardize our results by expressing the homogenates in units of mg protein/ml instead of g liver/ml. In addition, the effects of long-term perfusion on receptor number were determined in the absence of EGF (▲, ▲). When standard error bars are present, the value is an average  $\pm$  SEM of at least four measurements. All other data points represent a single determination.

during steady state (Fig. 7). Latent receptors remained at  $\sim 230,000/\text{cell}$  for up to 2 h and then declined to  $150,000/\text{cell}$  at 4 h. Furthermore, the number of total receptors remained the same for up to 2 h despite the degradation of substantial amounts of EGF during this time. Throughout the next 2 h, only 0.3 receptor sites were inactivated per molecule of EGF degraded (90,000 receptors lost per cell vs. 320,000 molecules degraded per cell, Fig. 8).

When livers were perfused in the absence of EGF for 4 h and the receptors were quantitated (Fig. 8), accessible receptors decreased to  $210,000/\text{cell}$  (70% of initial), but total receptor number remained virtually unchanged ( $280,000 \pm 36,000$  receptors per cell). Therefore, the decrease in receptor number was due to the presence of EGF not cell dysfunction brought about by the perfusion conditions. However, 30% of the initially accessible receptors were transferred to a latent pool even in the absence of ligand.

### Subcellular Distribution of EGF and Its Receptor

Livers were perfused with  $^{125}\text{I}$ -EGF either at  $4^\circ\text{C}$  for 90 min (to label the cell surface), at  $35^\circ\text{C}$  for 10–20 min when ligand degradation was not yet evident (to label the contents of endosomes I–III), or at  $35^\circ\text{C}$  for 120 min when ligand degradation was occurring (to possibly label the contents of lysosomes). Livers were then homogenized and three fractions were prepared: material sedimenting at  $12,000 \text{ g}$  (the 12-K fraction) or at  $145,000 \text{ g}$  (the microsomal fraction), and material remaining in the  $145,000 \text{ g}$  supernatant (the cytosolic fraction). The 12-K and microsomal fractions were subfractionated on continuous sucrose gradients. The distributions of bound or sequestered EGF and of accessible and/or total EGF binding activities were determined in the three subcel-

lular fractions as well as in the sucrose gradients and compared with those of conventional enzyme markers for the plasma membrane (5'-NUC and APDE), Golgi apparatus (Gal-Trans), and lysosomes ( $\beta$ -NAG) (Figs. 9 and 10). Enzyme markers for plasma membrane and Golgi apparatus were equally distributed between the 12-K and microsomal fractions, while lysosomes were predominantly located in the 12-K fraction (80% of  $\beta$ -NAG activity). Less than 5% of any of the enzyme activities remained in the cytosolic fraction.

**DISTRIBUTION OF LIGAND AT 0–20 MIN AFTER EXPOSURE TO EGF:** When fractions from livers exposed to  $^{125}\text{I}$ -EGF at  $4^\circ\text{C}$  (surface-bound) were examined,  $\sim 20\%$  of the ligand did not sediment, suggesting release. However, the remaining 80% was equally divided between the two sedimentable fractions. As described in the morphology section, 10–25 min after exposure to EGF-HRP, many endosomes (II + III) containing ligand were located within the peribiliary region (Table I and Fig. 5). Fractionation of homogenates from comparable livers exposed to  $^{125}\text{I}$ -EGF for 10–20 min revealed that 78–96% of the homogenate radioactivity was associated with vesicles that sedimented at  $12,000 \text{ g}$  (20–51%) or  $145,000 \text{ g}$  (45–58%). The equal distribution of bound or sequestered ligand between the 12-K and microsomal fractions was not coincident with  $\beta$ -NAG activities but did resemble that seen for Gal-Trans, 5'-NUC, and APDE activities.

The heterogeneous composition of the two sedimentable fractions prompted us to resolve the different subpopulations (i.e., plasma membrane, lysosomes, Golgi apparatus, and endosomes) by isopycnic centrifugation on sucrose gradients (Figs. 9 and 10). The distribution of surface-bound EGF (i.e., 90 min,  $4^\circ\text{C}$ ) was examined first.  $^{125}\text{I}$ -EGF that sedimented with the microsomal fraction equilibrated as a single band on sucrose gradients at a peak density of  $1.15 \text{ g/cc}$  (Fig. 10). This



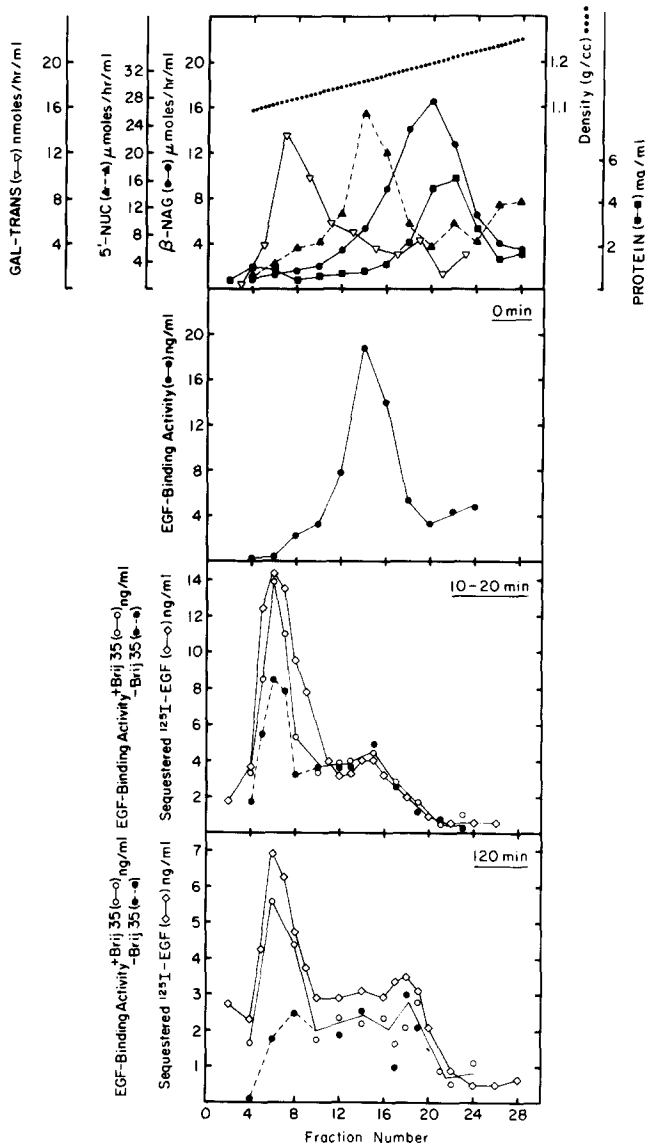


FIGURE 9 Distribution on sucrose gradients of sequestered EGF and of EGF receptors in the 12-K fraction. Livers were either perfused with saline (0 min, control) or perfused at 35°C with 20 nM  $^{125}\text{I}$ -EGF for 10–20 min or 120 min. 12-K fractions were obtained and further fractionated on continuous sucrose gradients as described in Materials and Methods. EGF-binding activity in 0.1-ml aliquots was measured in the absence or presence of detergent. Owing to the lower protein content in these samples as compared with liver homogenates, 0.2% Brij 35 was sufficient for measuring maximal EGF binding.

peak was coincident with that of the plasma membrane markers, 5'-NUC and APDE (latter enzyme not shown). We then examined the behavior of EGF-containing vesicles or endosomes (i.e., 10–20 min, 37°C) on sucrose gradients. 90% of the radioactivity applied entered the gradients and none coincided with the lysosomes (1.18–1.25 g/cc) (Figs. 9 and 10). Only ~20% of the radioactivity distributed at densities corresponding to the plasma membrane (1.14–1.17 g/cc, Figs. 9 and 10), which was consistent with the amount of residual  $^{125}\text{I}$ -EGF bound to the surface. At least 70% of the ligand-containing vesicles migrated at densities between 1.08 and 1.13 g/cc. These vesicles were well-separated from the bulk of the protein (80%) and from at least 70% of the 5'-NUC and

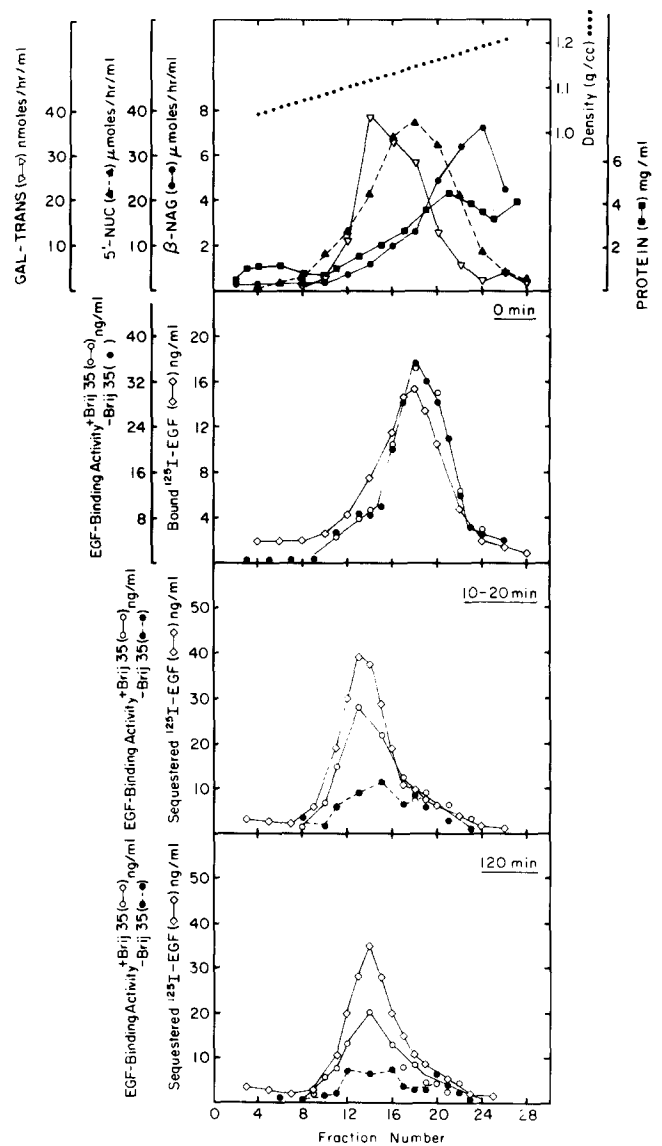


FIGURE 10 Distribution on sucrose gradients of sequestered EGF and of EGF receptors in the microsomal fraction. Livers were either perfused with saline (0 min, control), perfused at 4°C with 8 nM  $^{125}\text{I}$ -EGF for 90 min (0 min), or perfused at 35°C with 20 nM  $^{125}\text{I}$ -EGF for 10–20 min or 120 min. Microsomal fractions were obtained and further fractionated on continuous sucrose gradients as described in Materials and Methods. EGF-binding activity in 0.1-ml aliquots was measured in the absence or presence of 0.2% Brij 35.

APDE activities. The behavior of Gal-Trans activity was similar but not identical to that of endosomes. That is, Gal-Trans distributed at higher densities (1.11–1.16 g/cc) than those seen for the  $^{125}\text{I}$ -EGF-labeled endosomes. Although still contaminated with other organelles, a 10–20-fold purification of the endosomes was accomplished with this procedure.

**DISTRIBUTION OF LIGAND AT LATER TIMES:** When the subcellular distribution of sequestered  $^{125}\text{I}$ -EGF from livers exposed to the ligand for 120 min was examined, 30% of the homogenate radioactivity sedimented at 12,000 g and 48% at 145,000 g. Subfractionation on sucrose gradients revealed that the bulk of the sequestered  $^{125}\text{I}$ -EGF at these later times was still in endosomes, not in lysosomes. Of the radioactivity present in the 12-K fractions, 40% equilibrated at densities of 1.08–1.13 g/cc, 29% at 1.14–1.17 g/cc (i.e., plasma membrane), and only 21% (6% of liver radioactivity)

at 1.18–1.25 g/cc (i.e., lysosomes). The <sup>125</sup>I-EGF in the microsomal fraction was distributed between the endosome-rich peak (70%) and the plasma membrane peak (20%).

**SUBCELLULAR DISTRIBUTION OF EGF-BINDING ACTIVITY BEFORE AND AFTER EGF EXPOSURE:** We first examined EGF receptor distribution in livers that had not been exposed to ligand. 85–90% of the EGF receptor was sedimentable and accessible to ligand binding (i.e., EGF binding ± detergent was the same). The membrane-associated receptor was equally distributed between the 12-K and microsomal fractions. Analysis of these fractions on sucrose gradients (Figs. 9 and 10) revealed in both cases that EGF-binding activity coincided with the plasma membrane marker enzymes (5'-NUC and APDE). Over 80% of the total binding activity applied to the sucrose gradient could be recovered and only 5% of this activity failed to enter the gradient.

After exposure of livers to EGF for only 10–20 min, as much as 80% of the total receptors were localized to a latent pool (Fig. 8). When total EGF binding (i.e., nonlatent and latent) was measured in fractions from liver homogenates prepared 10–20 or 120 min after EGF addition, 20–50% sedimented at 12,000 g, 45–58% sedimented at 145,000 g, and <5% was nonsedimentable. When the 12-K and microsomal fractions were analyzed on sucrose gradients, we found that the receptors had shifted to a lighter density (1.08–1.13 g/cc, Figs. 9 and 10). As much as 70% of the total EGF-binding activity recovered now co-localized with the EGF-containing vesicles, not with the plasma membrane. Of the receptors that equilibrated in this region of the gradient (i.e., endosomes), 40–80% displayed latency. In contrast, the bulk of the accessible receptors (20% of the total receptors) equilibrated with the plasma membrane markers and presumably represented those receptors still at the cell surface.

At 120 min but not 10–20 min after EGF addition, a small fraction of the EGF-binding activity was detected at densities corresponding to lysosomes (1.18–1.25 g/cc, Fig. 9). However, due to the limitations of the binding assay, samples with a low capacity to bind EGF (<3 ng EGF bound/ml) were difficult to measure accurately. For this reason the presence of EGF receptors in the lysosomes could not be demonstrated conclusively.

#### *Effects of Leupeptin on the Metabolism of <sup>125</sup>I-EGF*

We found little EGF accumulating in hepatic lysosomes at any time despite extensive hydrolysis of the ligand. Although a similar result for asialofetuin has been reported (23), indicating a very efficient lysosomal system in hepatocytes, we wanted to determine whether lysosomes were responsible for the degradation of EGF. Therefore, we used leupeptin, a proteinase inhibitor that has been shown to inhibit the degradation of asialofetuin resulting in its accumulation in lysosomes (23). We found that 0.4 mM leupeptin had no effect on EGF uptake but inhibited the rate of release of acid-soluble radioactivity by as much as 80%. In the presence of leupeptin, there were 340,000 molecules of EGF per hepatocyte at 2 h and 440,000 molecules per hepatocyte at 4 h, as compared with 200,000 molecules in the untreated cell at steady-state. Subcellular fractionation of leupeptin-treated livers revealed an increase in EGF content in the 12-K and cytosolic fractions (Table II). The increased level of EGF present in this latter fraction was probably due to breakage during homogenization

TABLE II  
Effect of Leupeptin on the Subcellular Distribution of <sup>125</sup>I-EGF in the Liver\*

Experiment	Fraction	Sucrose gradient (g/cc)			
		1.08–1.13 (Endo- somes)	1.14–1.17 (Plasma mem- branes)	1.18– 1.25 (Lys- somes)	
		μg EGF	μg EGF	μg EGF	μg EGF
Control	12 K	0.52	0.26	0.20	0.13
	Microsomal	0.87			
	Cytosolic	0.17			
	Total	1.70			
Leupeptin	12 K	1.95	0.58	0.42	0.94
	Microsomal	0.90			
	Cytosolic	0.91			
	Total	3.94			

\* Isolated livers were perfused in the absence or presence of leupeptin (0.4 mM) for 15 min before addition of <sup>125</sup>I-EGF (15 nM). After 2 h of perfusion at 35°C, the livers were homogenized in cold SI and separated into the three fractions indicated. The acid-insoluble radioactivity in these fractions and in the total homogenate were then determined and expressed as micrograms of EGF. The 12-K fraction was analyzed on sucrose gradients, the <sup>125</sup>I found in the density ranges corresponding to endosomes, plasma membranes, and lysosomes (see Fig. 9) was determined, and the results were expressed as micrograms of EGF.

of the enlarged lysosomes in leupeptin-treated livers (45). Analysis of the 12-K fraction on a sucrose gradient revealed that 50% of the <sup>125</sup>I-EGF migrated in the density range of lysosomes (1.18–1.25 g/cc, Fig. 9). Furthermore, the amount of <sup>125</sup>I-EGF co-migrating with lysosomes in leupeptin-treated livers was increased sevenfold over that of controls (Table II).

#### DISCUSSION

In this study, we have demonstrated that rat hepatocytes possess many EGF receptors that mediate the endocytosis of substantial amounts of circulating EGF. We found that EGF is internalized and transported to lysosomes via the same pathway as that used by other ligands destined for hydrolysis in hepatocytes. Concomitant with the initial wave of EGF internalization there is the redistribution of an equivalent number of receptors from the cell surface to endosomes but apparently not to lysosomes. However, unlike the ligand, which is degraded, our results suggest that a majority of the internalized receptors are reutilized. Furthermore, indirect evidence presented here suggests that at steady state the rates of uptake and degradation of EGF are dependent on the rate of receptor insertion into the plasma membrane and the rate of endosome/lysosome fusion, respectively.

#### *Exposure to EGF Induces a Rapid Disappearance of Cell Surface EGF Receptors*

We measured 150,000 receptors per cell in the perfused liver and 300,000 receptors per cell in vitro. At present we don't understand the basis for this two-fold difference, but we believe, for several reasons, that the increased number found in liver homogenates represents receptors at the plasma membrane and not those in an intracellular pool. First, the binding in naive cells displays no latency, whereas we can detect latent receptors in cells actively endocytosing EGF. Second, all the binding activity in naive cells migrates on sucrose gradients with conventional plasma membrane markers, not internal

membrane markers. Finally, the initial rapid wave of EGF clearance results in the uptake of about 300,000 ligand molecules, suggesting that all the receptors detected in vitro (300,000/cell) are in a functionally equivalent pool or site.

Upon addition of EGF to a perfused liver, we observed a rapid and dramatic disappearance of cell surface EGF receptors that closely paralleled the internalization of ligand in both time and extent. The number of surface receptors decreased by 80% within 20 min and remained at this low level for up to 4 h. Furthermore, the observed down-regulation of EGF receptors at the surface coincided with the appearance of an internal pool of receptors having the biochemical characteristics of endosomes. Thus, one wave of EGF internalization was sufficient to induce a massive redistribution of receptors and to establish a new equilibrium such that only 20% of the EGF receptors remained at the cell surface and 80% were within endosomes.

Receptor down-regulation has been described previously for EGF as well as for hormones (e.g., insulin [12, 13]) in hepatocytes and other cells (7–11). However, the mechanism(s) of EGF receptor down-regulation (redistribution and/or degradation) have not yet been resolved. Das and Fox (8) and Krupp et al. (10) concluded that receptor degradation accounted for down-regulation in 3T3 and A431 cells, respectively. In contrast, Wiley and Cunningham (11) used a mathematical modeling approach to analyze EGF endocytosis at steady state in 3T3 cells and concluded that down-regulation was the result of an increased rate of receptor internalization. We were able to follow the EGF receptor into the cell and demonstrate that down-regulation in hepatocytes was due to a rapid and substantial redistribution, not degradation, of receptors.

### *Pre-existing EGF Receptors Are Reutilized*

We found that hepatocytes were able to internalize and degrade EGF well in excess of total functional receptors. Since this occurred in the absence of new receptor synthesis, reutilization of pre-existing receptors must have occurred. Receptor reutilization has been implicated in the endocytosis of several other ligands, such as  $\alpha_2$ -macroglobulin–protease complexes and mannose glycoconjugates in alveolar macrophages (46, 47), LDLs lipoproteins in fibroblasts (1, 5), and ASGPs and insulin in liver (6, 48). However, the evidence that receptors actually disappear from the cell surface in the process of internalizing ligand and then return (i.e., recycle) for further rounds of internalization is still indirect. Our observations that surface EGF receptors are initially internalized into vesicles similar to endosomes and continue to be found in these vesicles during the steady state that follows, together with our evidence for reutilization, suggest strongly that EGF receptors are recycled between surface and intracellular sites.

The processes required for return of internalized receptors to the plasma membrane are (a) dissociation of the ligand-receptor complex; (b) separation of the receptor from ligand-containing vesicles; (c) transport to the plasma membrane; and (d) insertion. We have shown that dissociation of the EGF receptor complex can occur at low pH (Fig. 2A), an environment that exists in endosomes of other cells (49, 50) and lysosomes of liver (51). The observation of Fitzgerald et al. (52) that EGF was released into the cytosol when adenovirus induced endosome lysis suggests that the ligand had dissociated from its receptor while in a prelysosomal compartment. In contrast, on the basis of a close association of

internalized EGF-ferritin with the membrane, McKanna et al. (53) suggested that EGF remained bound to its receptor until entry into lysosomes. We have found that the amount of EGF internalized by hepatocytes at 16°C, a temperature that inhibits endosome–lysosome fusion in liver (24), is limited and equals the total complement of EGF receptors, that surface receptors are depleted by >90% at 16°C, and that an equivalent number of latent receptors appears in endosomes at this temperature (W. A. Dunn and A. L. Hubbard, unpublished observations). These results suggest that entry of the EGF receptor into lysosomes (whether bound to ligand or free) may be a prerequisite for recycling. Furthermore, the existence of large amounts of undegraded EGF, apparently together with receptor in endosomes at steady state at 37°C, again suggests that entry into lysosomes may be the rate-limiting step for both EGF degradation and for the return of receptor to the plasma membrane. An alternate possibility which might account for the excess of EGF internalized over receptors measured would be activation of previously inactive receptors in response to EGF exposure. However, until immunological reagents are obtained and the existence of an inactive pool of receptors in hepatocytes can be evaluated, we believe receptor reutilization and recycling adequately explain our data.

After the initial wave of receptor and EGF internalization, we found that the number of surface receptors in hepatocytes remained constant despite continued EGF endocytosis. Thus, the rate of insertion of recycling receptors from the internal pool must have equaled the rate of EGF uptake, which was 2,500 molecules/min per cell. Since the clearance rate of EGF at steady state appeared to be zero-order, either insertion of unoccupied receptor or internalization of the ligand–receptor complex must have been rate limiting, not binding of EGF to receptor, at least at the saturating EGF concentrations we used. Wiley and Cunningham (11) estimated that 320 EGF receptors were inserted into the plasma membrane per min per cell at steady state in fibroblasts, but the origin of these receptors (recycled vs. newly synthesized) was not determined. From our studies with the perfused liver we conclude that receptor recycling is occurring during the continual uptake of EGF and propose that the rate of ligand clearance at steady state is governed by the rate of insertion of receptors into the plasma membrane. Furthermore, this rate must be 2,500/min per cell, a value 10 times higher than that calculated for EGF receptor insertion in fibroblasts (11).

### *Degradation of EGF by Hepatocytes*

What is the evidence that EGF is degraded within lysosomes? Since this ligand was hydrolyzed rapidly by hepatocytes once it reached a degradative compartment, it was difficult to detect significant amounts of intact or even partially degraded  $^{125}\text{I}$ -EGF within these structures. Similar observations were reported for asialofetuin (23). However, we found that leupeptin, a potent inhibitor of lysosomal cathepsins B and L (54), inhibited EGF degradation by 80% resulting in the accumulation of ligand in lysosomes. In addition, other studies have reported EGF entry into structures identified morphologically as lysosomes (18, 53). Thus, we believe EGF hydrolysis occurs within lysosomes subsequent to their fusion with endosomes.

Our cytochemical experiments with EGF-HRP revealed that ligand was transported rapidly from the surface to endosomes in the Golgi apparatus–lysosome region of hepatocytes

( $t_{1/2} \cong 7-8$  min). However, no degradation of ligand was detected for at least 20 min. Subfractionation of livers exposed to EGF for 10–20 min demonstrated both ligand and receptor to be in endosomes not lysosomes. Thus, it would appear that the delay in entry of ligand into lysosomes is not due to transport but rather some obligate aging process of endosomes II + III, possibly influenced by ligand and/or receptor which renders the endosome (or some derivative) competent to fuse with lysosomes. In agreement with such a proposal, we found that the hydrolysis of ligand was linear with time at all levels of EGF added, suggesting that this step was governed by a cellular event that occurred at a constant rate, perhaps entry into lysosomes. Furthermore, at subsaturating EGF concentrations ( $<14$  nM), the rates of hydrolysis were proportional to the primary rates of ligand internalization but were approximately  $1/10$  those rates. These last two observations are consistent with the possibility that a constant number of endosomes (or some derivative) fuse with lysosomes at a constant rate, regardless of their content of EGF. This possibility is currently being investigated.

We would like to thank Ms. Susan Cameron for assistance with EGF-HRP cytochemistry, Mr. Tom Urquhart for photographic work, and Ms. Arlene Daniel for preparation of this manuscript. In addition, we would like to thank Dr. Reid Townsend for his assistance with the computer analysis of our ligand binding results.

This work was supported by a grant from the National Institutes of Health (GM29133) to A. Hubbard and from the National Science Foundation (PDF-8166053) to W. Dunn.

Received for publication 28 September 1983, and in revised form 17 February 1984.

## REFERENCES

- Goldstein, J. L., R. G. W. Anderson, and M. S. Brown. 1979. Coated pits, coated vesicles, and receptor-mediated endocytosis. *Nature (Lond.)* 279:679–685.
- Ashwell, G., and J. Harford. 1982. Carbohydrate-specific receptors of the liver. *Annu. Rev. Biochem.* 51:531–554.
- Roth, T. F., J. A. Cutting, and S. B. Atlas. 1976. Protein transport: a selective membrane mechanism. *J. Supramol. Struct.* 4:527–548.
- Mullock, B. M., and R. H. Hinton. 1981. Transport of proteins from blood to bile. *Trends Biochem. Sci.* 6:188–191.
- Goldstein, J. L., S. K. Basu, G. Y. Brunschede, and M. S. Brown. 1976. Release of low density lipoprotein from its cell surface receptor by sulfated glycosaminoglycans. *Cell* 7:85–95.
- Steer, C. J., and G. Ashwell. 1980. Studies on a mammalian hepatic binding protein specific for asialoglycoproteins. Evidence for receptor recycling in isolated rat hepatocytes. *J. Biol. Chem.* 255:3008–3013.
- Carpenter, G., and S. Cohen. 1976.  $^{125}$ I-labeled human epidermal growth factor: binding, internalization, and degradation in human fibroblasts. *J. Cell Biol.* 71:159–171.
- Das, M., and C. F. Fox. 1978. Molecular mechanism of mitogen action: processing of receptor induced by epidermal growth factor. *Proc. Natl. Acad. Sci. USA.* 75:2644–2648.
- Moriarty, D. M., and C. R. Savage, Jr. 1980. Interaction of epidermal growth factor with adult rat liver parenchymal cells in primary culture. *Arch. Biochem. Biophys.* 203:506–518.
- Krupp, M. N., D. T. Connolly, and M. D. Lane. 1982. Synthesis, turnover, and down-regulation of epidermal growth factor receptors in human A431 epidermoid carcinoma cells and skin fibroblasts. *J. Biol. Chem.* 257:11489–11496.
- Wiley, H. S., and D. D. Cunningham. 1981. A steady state model for analyzing the cellular binding, internalization and degradation of polypeptide ligands. *Cell* 25:433–440.
- Krupp, M., and M. D. Lane. 1981. On the mechanism of ligand-induced down-regulation of insulin receptor level in the liver cell. *J. Biol. Chem.* 256:1689–1694.
- Desbuquois, B., S. Lopez, and H. Burlet. 1982. Ligand-induced translocation of insulin receptors in intact rat liver. *J. Biol. Chem.* 257:10852–10860.
- Hubbard, A. L., G. Wilson, G. Ashwell, and H. Stukenbrok. 1979. An electron microscope autoradiographic study of the carbohydrate recognition systems in rat liver. I. Distribution of  $^{125}$ I-ligands among the liver cell types. *J. Cell Biol.* 83:47–64.
- Carpentier, J.-L., P. Gorden, P. Barazzone, P. Freychet, A. LeCam, and L. Orci. 1979. Intracellular localization of  $^{125}$ I-labeled insulin in hepatocytes from intact rat liver. *Proc. Natl. Acad. Sci. USA.* 76:2803–2807.
- Iwanij, V. 1980. Intracellular pathway of  $^{125}$ I-glucagon in the rat liver. *J. Cell Biol.* 87(2, Pt. 2):172a (Abstr.).
- Josefsberg, Z., B. I. Posner, B. Patel, and J. J. M. Bergeron. 1979. The uptake of prolactin into female rat liver. Concentration of intact hormone in the Golgi apparatus. *J. Biol. Chem.* 254:209–214.
- St. Hilaire, R. J., and A. L. Jones. 1982. Epidermal growth factor: its biologic and metabolic effects with emphasis on the hepatocyte. *Hepatology (Baltimore)* 2:601–613.
- Burger, R. L., R. J. Schneider, C. S. Mehlman, and R. H. Allen. 1975. Human plasma R-type vitamin B<sub>12</sub>-binding proteins. *J. Biol. Chem.* 250:7707–7713.
- Higa, Y., S. Oshiro, K. Kino, H. Tsunoo, and H. Nakajima. 1981. Catabolism of globin-haptoglobin in liver cells after intravenous administration of hemoglobin-haptoglobin to rats. *J. Biol. Chem.* 256:12322–12328.
- Smith, A., and W. T. Morgan. 1981. Hemopexin-mediated transport of heme into isolated rat hepatocytes. *J. Biol. Chem.* 256:10902–10909.
- Prieels, J. B., S. V. Pizzo, L. R. Glasgow, J. C. Paulson, and R. L. Hill. 1978. Hepatic receptor that specifically binds oligosaccharides containing fucosyl  $\alpha$ 1-3 N-acetylglucosamine linkages. *Proc. Natl. Acad. Sci. USA.* 75:2215–2219.
- Dunn, W. A., J. LaBadie, and N. N. Aronson, Jr. 1979. Inhibition of  $^{125}$ I-asialofetuin catabolism by leupeptin in the perfused rat liver and in vivo. *J. Biol. Chem.* 254:4191–4196.
- Dunn, W. A., A. L. Hubbard, and N. N. Aronson, Jr. 1980. Low temperature selectively inhibits fusion between pinocytotic vesicles and lysosomes during heterophagy of  $^{125}$ I-asialofetuin by the perfused rat liver. *J. Biol. Chem.* 255:5971–5978.
- Wall, D. A., G. Wilson, and A. L. Hubbard. 1980. The galactose-specific recognition system of mammalian liver: the route of ligand internalization in rat hepatocytes. *Cell* 21:79–93.
- Dunn, W. A., D. A. Wall, and A. L. Hubbard. 1983. Use of the isolated, perfused liver in studies of receptor-mediated endocytosis. *Methods Enzymol.* 98:225–240.
- Dunn, W. A., and A. L. Hubbard. 1982. Receptor mediated endocytosis of epidermal growth factor by liver. *J. Cell Biol.* 95(2, Pt. 2):425a (Abstr.).
- Savage, C. R., Jr., and S. Cohen. 1972. Epidermal growth factor and a new derivative. Rapid isolation procedures and biological and chemical characterization. *J. Biol. Chem.* 247:7609–7611.
- Taylor, J. M., W. M. Mitchell, and S. Cohen. 1972. Epidermal growth factor. Physical and chemical properties. *J. Biol. Chem.* 247:5928–5934.
- Greenwood, F., W. Hunter, and J. Glover. 1963. The preparation of  $^{131}$ I-labeled human growth hormone of high specific activity. *Biochem. J.* 89:114–123.
- Krebs, H. A., N. W. Cornell, P. Lund, and R. Hems. 1974. Isolated liver cells as experimental material. In *Regulation of Hepatic Metabolism*. F. Lundquist and N. Tygstrup, editors. Munksgaard, Copenhagen. 726–750.
- Carpenter, G. 1979. Solubilization of membrane receptor for epidermal growth factor. *Life Sci.* 24:1691–1698.
- Sell, S., D. S. Linthicum, D. Bass, R. Bahu, B. Wilson, and P. Nakane. 1977. Immunohistologic techniques. In *Advances in Pathobiology: Differentiation and Carcinogenesis*. Vol. IV. C. Borek, C. M. Fenoglio, and D. W. King, editors. Stratton Intercontinental Medical Book Corp., NY. 272–305.
- Hubbard, A. L., and Z. A. Cohn. 1972. The enzymatic iodination of the red cell membrane. *J. Cell Biol.* 55:390–405.
- Howell, K. E., A. Ito, and G. E. Palade. 1978. Endoplasmic reticulum marker enzymes in Golgi fractions—what does this mean? *J. Cell Biol.* 79:581–589.
- LaBadie, J. H., K. P. Chapman, and N. N. Aronson, Jr. 1975. Glycoprotein catabolism in rat liver. Lysosomal digestion of iodinated asialo-fetuin. *Biochem. J.* 152:271–279.
- Bradford, M. 1976. A rapid and sensitive method for the quantitation of microgram quantities of protein utilizing the principle of protein-dye binding. *Anal. Biochem.* 72:248–254.
- Hubbard, A. L., D. A. Wall, and A. Ma. 1983. Isolation of rat hepatocyte plasma membranes. I. Presence of the three major domains. *J. Cell Biol.* 96:217–229.
- Beaufay, H., A. Amar-Costesec, E. Feytmans, D. Thines-Sempoux, M. Wibo, M. Robbi, and J. Berthet. 1974. Analytical study of microsomes and isolated subcellular membranes from rat liver. I. Biochemical methods. *J. Cell Biol.* 61:188–200.
- Munson, P. J., and D. Rodbard. 1980. Ligand: a versatile computerized approach for characterization of ligand-binding systems. *Anal. Biochem.* 107:220–239.
- Helenius, A., I. Mellman, D. Wall, and A. Hubbard. 1983. Endosomes. *Trends Biochem. Sci.* 8:245–250.
- Hubbard, A. L., D. A. Wall, and W. A. Dunn. 1983. The intracellular pathway taken by asialoglycoproteins and epidermal growth factor in rat hepatocytes. In *Structural Carbohydrates in the Liver*. H. Popper, W. Reutter, F. Gudat, and E. Kottgen, editors. MTP Press Limited, Boston. 265–275.
- Silverstein, S. C., R. M. Steinman, and Z. A. Cohn. 1977. Endocytosis. *Annu. Rev. Biochem.* 46:669–722.
- Khairallah, E. A., and G. E. Mortimore. 1976. Assessment of protein turnover in perfused rat liver. Evidence for amino acid compartmentation from differential labeling of free and tRNA-bound valine. *J. Biol. Chem.* 251:1375–1384.
- Aronson, N. N., Jr., P. A. Dennis, and W. A. Dunn. 1981. Metabolism of leupeptin and its effect on autophagy in the perfused rat liver. *Acta Biol. Med. Ger.* 40:1531–1538.
- Kaplan, J. 1980. Evidence for reutilization of surface receptors for  $\alpha$ -macroglobulin-protease complexes in rabbit alveolar macrophages. *Cell* 19:197–205.
- Stahl, P., P. H. Schlesinger, E. Sigardson, J. S. Rodman, and Y. C. Lee. 1980. Receptor-mediated pinocytosis of mannose glycoconjugates by macrophages: characterization and evidence for receptor recycling. *Cell* 19:207–215.
- Fehlmann, M., J.-L. Carpentier, E. Van Obberghen, P. Freychet, P. Thamm, D. Saunders, D. Brandenburg, and L. Orci. 1982. Internalized insulin receptors are recycled to the cell surface in rat hepatocytes. *Proc. Natl. Acad. Sci. USA.* 79:5921–5925.
- Tycko, B., and F. R. Maxfield. 1982. Rapid acidification of endocytic vesicles containing  $\alpha$ 2-macroglobulin. *Cell* 28:643–651.
- Galloway, C. J., G. E. Dean, M. Marsh, G. Rudnick, and I. Mellman. 1983. Acidification of macrophage and fibroblast endocytic vesicles in vitro. *Proc. Natl. Acad. Sci. USA.* 80:3334–3338.
- Ohkuma, S., Y. Moriyama, and T. Takano. 1982. Identification and characterization of a protein pump on lysosomes by fluorescein isothiocyanate-dextran fluorescence. *Proc. Natl. Acad. Sci. USA.* 79:2758–2762.
- Fitzgerald, D. J., P. R. Padmanabhan, I. Pastan, and M. C. Willingham. 1983. Adenovirus-induced release of EGF and pseudomonas toxin into the cytosol of KB cells during receptor mediated endocytosis. *Cell* 32:607–617.
- McKanna, J. A., H. T. Haigler, and S. C. Cohen. 1979. Hormone receptor topology and dynamics: morphological analysis using ferritin-labeled epidermal growth factor. *Proc. Natl. Acad. Sci. USA.* 76:5689–5693.
- Barrett, A. J. 1979. Cathepsin B and other thiol proteinases. In *Proteinases in Mammalian Cells and Tissues*. A. J. Barrett, editor. Elsevier/North Holland, NY. 181–208.